Quantum resonance of nanometre-scale metal-ZnO-metal structure and its application in sensors

Lijie Li and Paul Rees

Citation: AIP Advances **6**, 015003 (2016); doi: 10.1063/1.4939815
View online: http://dx.doi.org/10.1063/1.4939815
View Table of Contents: http://scitation.aip.org/content/aip/journal/adva/6/1?ver=pdfcov
Published by the AIP Publishing

Quantum resonance of nanometre-scale metal-ZnO-metal structure and its application in sensors

Lijie Li[a] and Paul Rees
College of Engineering, Swansea University, Swansea, Wales SA2 8PP, United Kingdom

(Received 27 October 2015; accepted 30 December 2015; published online 7 January 2016)

Analysis of the thickness dependence of the potential profile of the metal-ZnO-metal (MZM) structure has been conducted based on Poisson's equation and Schottky theory. Quantum scattering theory is then used to calculate the transmission probability of an electron passing through the MZM structure. Results show that the quantum resonance (QR) effect becomes pronounced when the thickness of the ZnO film reaches to around 6 nm. Strain induced piezopotentials are considered as biases to the MZM, which significantly changes the QR according to the analysis. This effect can be potentially employed as nanoscale strain sensors. © *2016 Author(s). All article content, except where otherwise noted, is licensed under a Creative Commons Attribution 3.0 Unported License.* [http://dx.doi.org/10.1063/1.4939815]

INTRODUCTION

Nanometer-scale structures thin films and nanowires exhibit different current-voltage characteristics to bulk, especially when the dimensions are comparable to the depletion thickness of the junction and the quantum length, i.e. de Broglie wavelength of an electron. Zinc oxide (ZnO) is one of ubiquitously used materials due to its unique performance exhibiting both semiconductor and piezoelectric characteristics. Devices such as varistors,[1] energy harvesters,[2] resistive switching devices,[3] and sensors[4] have all been fabricated in ZnO. In these applications, ZnO was used in various forms, including thin films, grains, nanowires, and nanorods. Particularly the ZnO nanostructures have very promising applications in mechanical-electrical energy harvesting, which has been reviewed in a great details in reference.[5] Other fields such as heterogeneous photocatalysis can also take the advantages of ZnO in terms of its low cost and high photoactivity. The photocatalytic performance could be significantly improved using graphene/ZnO nanocomposites.[6] A review has been given on the ZnO nanostructures being utilized in solar cells emphasising on dye-sensitized solar cells, quantum dot-sensitized solar cells, and integrated cells for simultaneously harvesting multiple-type energies.[7] Interesting findings using ZnO nanorods on single layer MoS2 has been reported to have enhanced Raman and photoluminescence emissions.[8] Owing to the piezoelectricity, ZnO nanorods can also be used to improve the photoresponse in Cu2/ZnO heterojunctions.[9] In nearly all these applications/devices it is the metal-ZnO (MZ) electrical junction that generates the important material properties. The MZ junction in general resembles a Schottky junction,[10] which can be explained by classic semiconductor theories. The Schottky junction of the MZ accompanied by piezoelectric characteristics is sometimes termed as piezotronics,[11,12] which has been attractive in shaping self-controlled transistors, sensors and actuators. Ever since the interesting performance of the ZnO was demonstrated, the material has been appearing intrinsically n-type. This work will first of all target on analyzing the depletion layer thickness to determine the critical thickness under which the potential profile starts to change its shape. Therefore dopant type and density should be carefully predefined. In this work it is assumed that the metal is contacting with a n-type ZnO film forming a MZ junction, in which electrons are induced on the metal-ZnO interface leaving holes in the depleted region of the ZnO body, which pulls down the conduction band to match the Fermi

[a]Email: L.Li@swansea.ac.uk

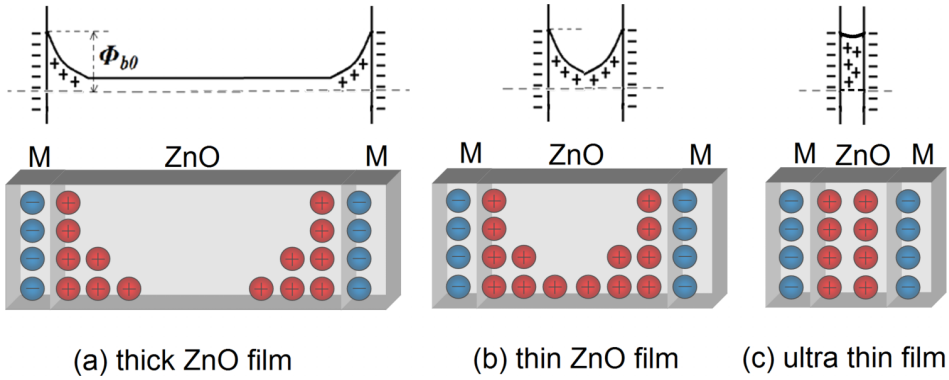

FIG. 1. schematic hypothesis of the size dependence effect of the metal-ZnO-metal structure. (a), Thickness of the ZnO film is much larger than the thickness of the depletion layer. (b), ZnO thickness is close to the depletion layer thickness. (c), Thickness of the film is much thinner than the depletion layer, causing the quantum confinement effect to appear.

level of the metal. The band diagram of the junction may change if the device dimension significantly reduces. The current voltage characteristics of the ZnO nanowires varying with the different diameters was observed in reference.[13,14] In this paper, it is aimed to unveil the physics of this phenomenon using combined semiconductor physics and quantum scattering theory to calculate the transmission probabilities and currents. Schematically shown in Figure 1 it is hypothesized that the critical thickness is when it approaches to the sum of the two depletion layers in the back-to-back Schottky junctions in the MZM structure. Further reducing the thickness, merged depletion layers lifts up the conduction band, eventually forming a quantum well. Here the band diagrams of the MZM for the thick, thin and ultra thin film have been calculated. After that, quantum scattering theory has been used to analyze the transmission coefficient of an electron passing through the MZM structure in relation to the electron energy.

I. SIZE DEPENDENCE OF SCHOTTKY BARRIER HEIGHT

From the semiconductor theory,[15] at the MZ interface, induced charges accumulate on the surface of the ZnO in order to match Fermi level of the metal, causing positive charges left behind in the body of ZnO. The region in the ZnO body containing remnant positive charges is the depletion layer. In the band diagram, the energy bands (conduction and valence) of the n-type ZnO film have bent down toward the bulk due to negative space charges accumulated on the surface of the film. The extent of band bending is determined by the barrier height formed in the MZ interface. To obtain the depletion thickness, assuming $x = 0$ at the surface of ZnO, N_D is the dopant density and x_d refers to the depletion depth to the bulk. The one dimensional Poisson's equation expressing the potential $V(x)$ within the depletion region $[0\ x_d]$ is

$$\frac{d^2V}{dx^2} = -\frac{e^2N_D}{\varepsilon_r\varepsilon_0}$$
$$V(x) = -\frac{e^2N_D}{2\varepsilon_r\varepsilon_0}(x - x_d)^2 \tag{1}$$

Normalization of V was chosen as $V = 0$ in the bulk beyond depletion region ($x > x_d$), and the boundary condition of $V(x_d) = 0$ is defined. The maximum potential V_m appears at the surface when $x = 0$, $V_m = -e^2N_Dx_d^2/2(\varepsilon_r\varepsilon_0)$. The depletion depth can be expressed as

$$x_d = \sqrt{\frac{2\varepsilon_r\varepsilon_0V_m}{e^2N_D}} \tag{2}$$

The maximum potential V_m is the barrier height subtracting the gap between the conduction band and Fermi band. In equilibrium, the chemical potential has to be the same everywhere. For MZ interface, the barrier height ϕ_{B0} has been reported in a very diverse range from (0.2 eV to

1.54 eV).[16–18] Here in this calculation we assign ϕ_{B0} as 0.7 eV. The value of relative permittivity ε_r of ZnO nanowire was reported to depending on its diameter[19] and in this work it is given 2.5 for the 100-150 nm thick film or nanowire diameter. Carrier concentration of ZnO nanowire was also reported in a very large range, 5.2×10^{23} m^{-3} is used in this work.[20] From equation (2), the depletion thickness x_d is calculated to be ~30 nm. In this study, temperature induced barrier height change is neglected as the electrical current is relatively small, and the device is placed in a good thermal conduction environment. The band diagram needs to be calculated firstly in order to conduct the quantum scattering analysis. Equations (1) and (2) are used to arrive at the band structure for various thicknesses. For n-type semiconductors, the barrier height is measured from the conduction band, hence only the conduction band is chosen in the analysis. Decreasing thicknesses from 100 nm to 5 nm, the calculated band diagram are shown in the Figure 2. It is seen that for the 100 nm thick film, the device is a typical back-to-back Schottky junction similar as reported in Ref. 21. When the film thickness is reduced to 30 nm (close to calculated depletion layer thickness) the whole film is dominated by the depletion layer. Further reducing the thickness to 5 nm, a rectangular shape energy diagram is formed, resembling a reversed finite potential well. It has been assumed that the charges number accumulated on the surface of the ZnO remains constant during the calculations. Quantum scattering theory is employed in the next section to account for the quantum confinement effect observed for thinner films.

II. CALCULATION OF TRANSMISSION PROBABILITY AND TUNNELING CURRENT FOR MZM WITH VARIOUS THICKNESSES

The quasi-rectangular potential profile formed by the thin ZnO film sandwiched by two metal electrodes is similar to a reversed quantum well; a potential profile spatially confines the electrons. Quantum theory describes that an electron in the quantum well has its energy quantized and a discrete energy spectrum would be expected. Quantum scattering theory is used to validate the energy quantization effect for the MZM structure with ultra thin ZnO film. In the classic theory, electrons can only pass a potential barrier if the electrons energy is higher than the barrier. However as the dimension of the device reduces to sufficiently small, the electrons treated as travelling waves can have the probability to tunnel through the barrier for those electrons with the energy corresponding approximately to the virtual resonant frequency level of the quantum well, in which case the transmission coefficient is close to unity. To calculate the transmission probability T_p for the thinned ZnO film, a well established method for electrons passing through arbitrary potential

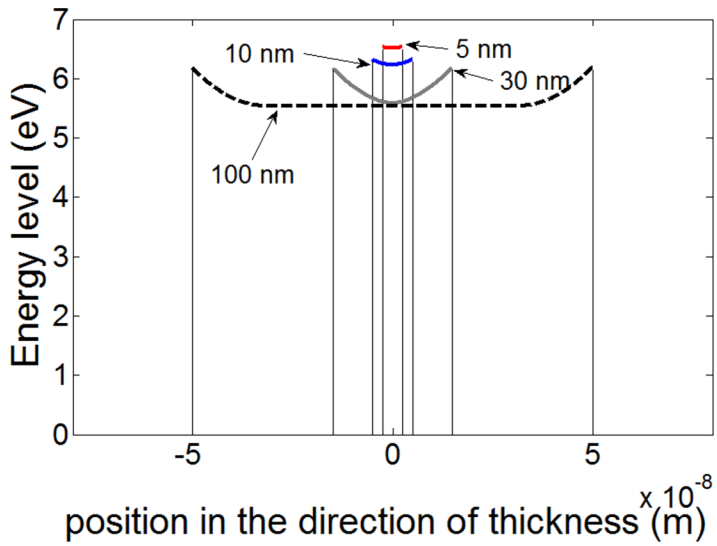

FIG. 2. Calculated results show energy bands of the MZM structure with various ZnO thicknesses.

profiles has been utilized.[22] The procedure can be briefly described as follows. The potential profile formed by the MZM structure has been segmented into N sections, each section is termed by j (j = 0, 1, 2, …, N-1, N). For an individual section of potential profile, the one dimensional wave function of an electron within the section j can be expressed by the Schrodinger equation

$$E\psi(x_j) + \frac{\hbar^2}{2m}\frac{d^2\psi(x_j)}{dx^2} = U(x_j)\psi(x_j) \tag{3}$$

where the E is the total energy of the electron, which is the combination of its initial energy and the energy caused by the externally applied voltage. The wave function ψ_j can be expressed as

$$\psi_j = A_j e^{ik_j x} + B_j e^{-ik_j x} \tag{4}$$

where $k_j = \sqrt{[2m(E - U(x_j))]}/\hbar$. The ψ_j and $d\psi_j/dz$ should be continuous at each boundary, then the amplitude A_j and B_j can be determined by the following equation:

$$\begin{pmatrix} A_j \\ B_j \end{pmatrix} = \prod_{l=0}^{j=1} M_l \begin{pmatrix} A_0 \\ B_0 \end{pmatrix} \tag{5}$$

where M_l is given by:

$$M_l = \begin{bmatrix} (1+S_l)\exp[-i(k_{l+1}-k_l)x_l] & (1-S_l)\exp[-i(k_{l+1}+k_l)x_l] \\ (1-S_l)\exp[i(k_{l+1}+k_l)x_l] & (1+S_l)\exp[i(k_{l+1}-k_l)x_l] \end{bmatrix} \tag{6}$$

Neglecting the change of electron mass, $S_l = k_l/k_l$+1.The scatting matrix M can then be obtained as:

$$M = \begin{bmatrix} M_{11} & M_{12} \\ M_{21} & M_{22} \end{bmatrix} = \prod_{l=0}^{N} M_l \tag{7}$$

Finally, by setting up the boundary condition, which is the initial incident wave set to the amplitude 1, and the reflection from the output terminal set to 0, i.e. A_0 =1 and B_{N+1} =0, the T_p can be calculated by: $T_p = \frac{k_{N+1}}{k_0}\left|\frac{k_0}{k_{N+1}M_{22}}\right|^2$. The transmission current can also be worked out using the equation $I_{out} = -q^2\frac{E}{\pi\hbar}T_p$. Because the calculate energy level from Figure 2 is within the range of 5 – 7 eV, the electron energy in this study is given 5 – 10 eV. Numerical calculation has been performed and the results for thicker film (50 nm & 100 nm) are shown in Figure 3. It is seen that as the electron

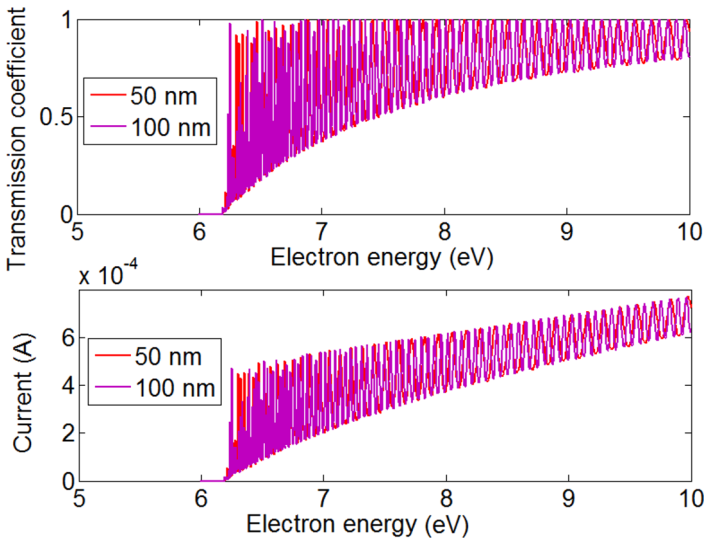

FIG. 3. Calculations of the electron transmission versus electron energy for film thickness of 50 nm and 100 nm.

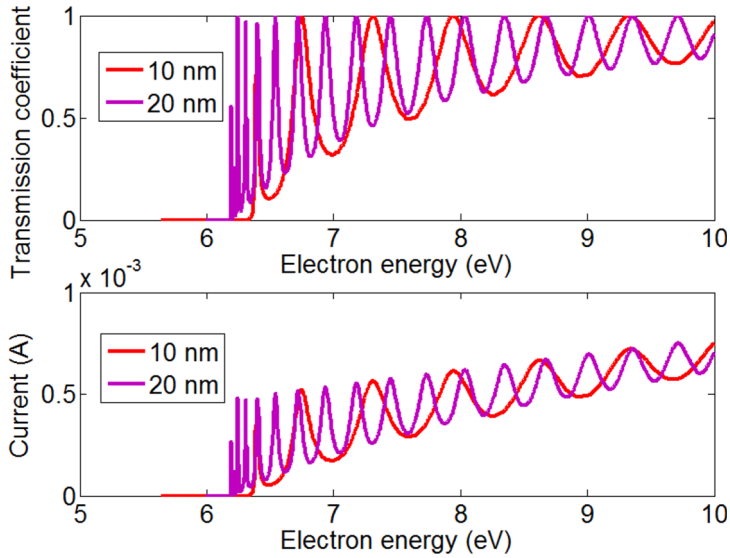

FIG. 4. Calculated results of the electron transmission versus electron energy for the MZM structure with much thicker films, 10 nm and 20 nm.

energy exceeds 6.2 eV, there is no obvious quantization of the electron energy; all the peaks in the T_p vs. E graph are very close to each other, which can be regarded as continuous. It means that electrons with energy above 6.2 eV can pass through the barrier. As the film gets thinner to 10 nm and 20 nm, the discrete energy levels appear in the high electron energy region (>6.5 eV), displayed in Figure 4. It manifests that only electrons having energy about the resonant energy levels can tunnel through. When the film is further thinned to 3 nm and 6 nm, the energy quantization effect dominates. Figure 5 shows that three resonant peaks are demonstrated for the 6 nm films and only one resonant peak is displayed for the 3 nm films. Interpreting the results in greater details, the first resonant peak of the T_p graph for thinner films has largest quality factor (Q), and the resonant tunneling lifetime $\tau = \frac{h^2}{4\pi\Delta\varepsilon_m}$($\Delta\varepsilon_m$ is the half-width of the resonant peak at half-maximum of the resonant peak around the resonance energy ε_m) can be used to characterize the energy uncertainty

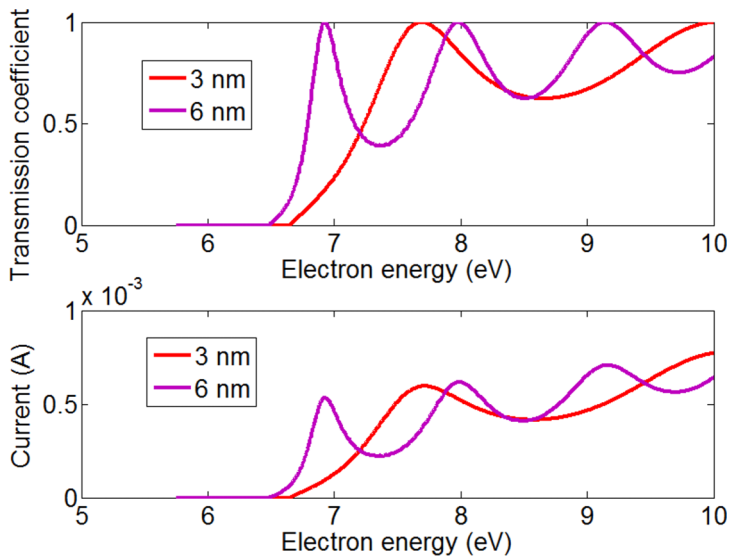

FIG. 5. Simulated results of the electron transmission probability and current against electron energy for 3 nm and 6 nm ZnO films respectively.

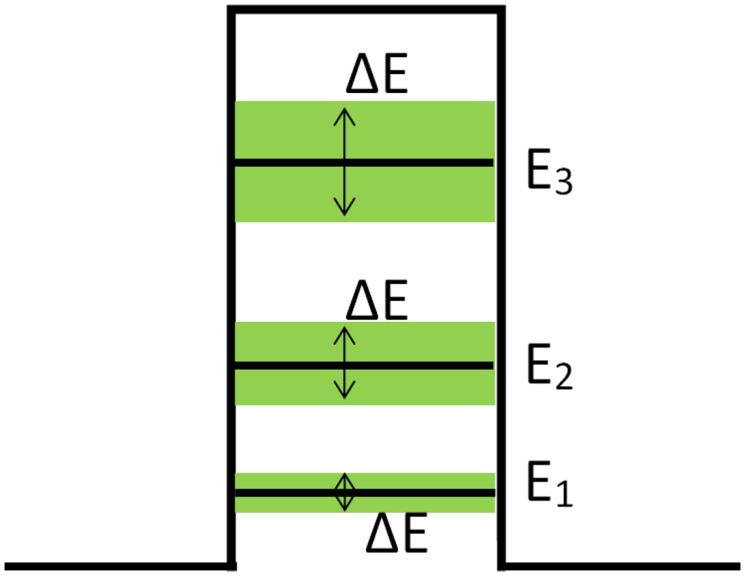

FIG. 6. The lowest resonant energy E1 has a narrower energy band, with energy in the band electrons have probability to pass through. Higher resonant peaks correspond to wider pass band.

condition at energy corresponding the resonating tunneling. Observing the results, the τ becomes smaller for higher resonant peaks, meaning the resonant curve similar to the Gaussian shape gets wider at higher energy resonances, where more electrons possessing energy in the larger range surrounding the resonant peak will have probability to tunnel through the barrier. This phenomenon is sketched in Figure 6, which matches the theory of the quantum resonance.[23]

III. QUANTUM TUNNELLING OF MZM STRUCTURE UNDER PIEZOELECTRIC POTENTIAL

For the particular material ZnO studied in this work, the piezoelectric property has been well demonstrated in the prior publications.[24] The phenomenon combining piezoelectric and electronics was termed as piezotronics. In this work, for the thinner ZnO film (6 nm) of MZM structure, quantum tunneling effect under the piezoelectric potential is investigated. A 0.5 V piezoelectric potential is chosen to be applied to the barrier. Previous publications show that 0.5 V output can be achieved from a single ZnO nanowire.[25] After the application of the piezopotential, the potential profile of the 6 nm is calculated as shown in Figure 7(a). Quantum scattering theory is used again for the biased barrier, and the result of the quantum resonance is shown in Figure 7(b). It is seen

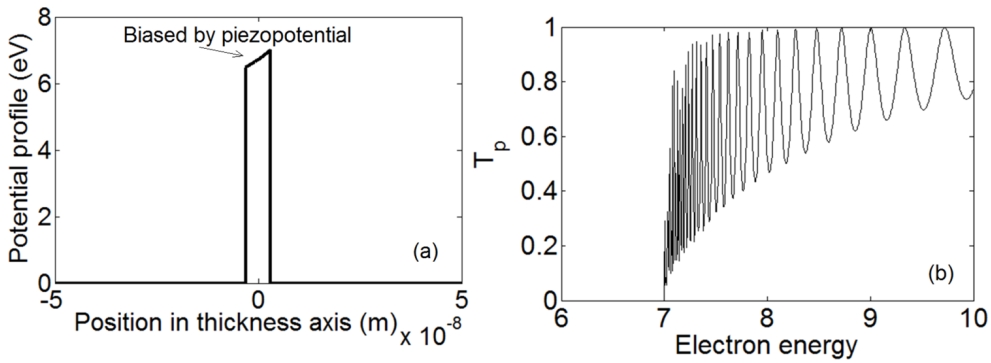

FIG. 7. Calculated results for biased MZM structure. 7a, 0.5 V biased potential profile for the 6 nm ZnO film. 7b, Simulated T_p versus electron energy for the biased MZM in 7a.

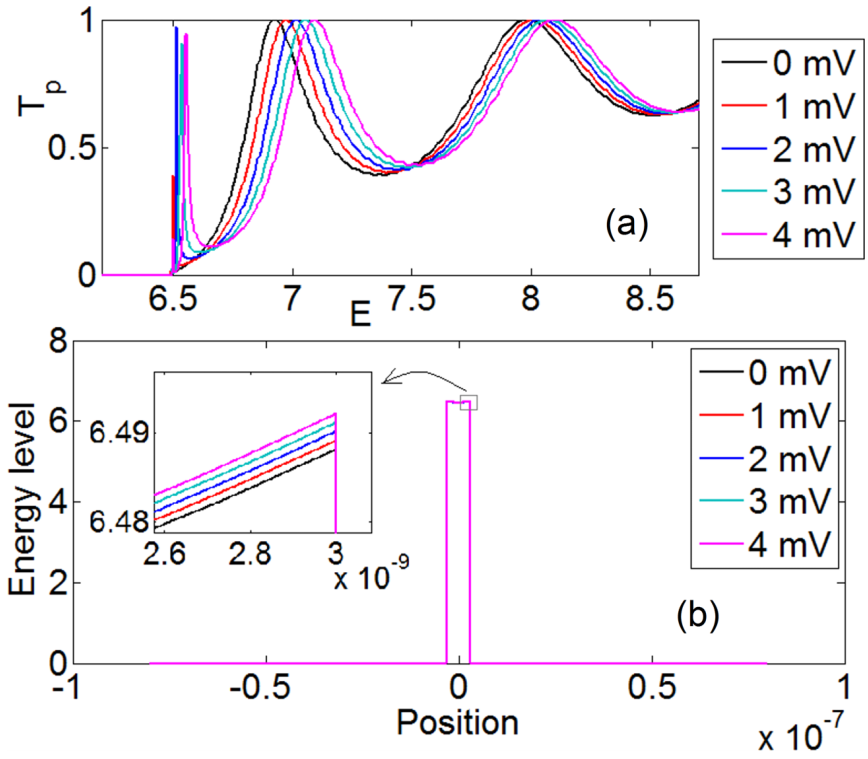

FIG. 8. Quantum resonance of the piezopotential biased MZM structure. 8a, T_p versus electron energy for the increasing bias. 8b, Potential profile for various piezopotentials, as the piezopotential is very small, inserted graph displays the details of the right corner of the potential profile.

that the main difference between the unbiased and biased quantum barrier is that the lower resonant peaks are no longer unity; implying electrons with the lower resonant energies don't have 100% transmission, which coincides with previous published results for biased quantum wells.[26] This phenomenon can be employed to construct a sensor device detecting mechanical strain changes in nanometer scale. To demonstrate the relation between the resonant peaks of T_p and the varied piezopotentials, numerical simulation has been conducted, and results are shown Figure 8. It can be seen that very small piezopotentials such as several mV induces significant changes in transmission probability. Specifically in this case study, as the piezopotential of 1 mV is present, there is a narrow resonance occurring at around 6.5 eV, and the first main resonant peak has shifted up by about 9% (from 6.92 eV to 6.98 eV). Further increasing the piezopotential to 4 mV, the first resonant peak has linearly rose to around 7.09 eV, corresponding a 25% increase. Moreover the narrow resonance appearing at around 6.5 eV has become more pronounced at higher piezopotentials. This phenomenon can be utilized to design high sensitivity nanoscale strain sensors. The sensors will be able to detect the strain change on a nanodevice where it is not possible for traditional detection methods.

IV. CONCLUSION

The quantum resonance has been observed in very thin ZnO film through theoretical simulations. The typical MZM structure has been investigated by using Poisson's equation and quantum scattering theory. It is shown that as the ZnO film is thinned to the scale comparable to the depletion thickness of the MZ junction, the quantum resonance effect starts to appear, which has been evidenced in the calculated transmission probability curves. Further study has been conducted to reveal the impact on the transmission probability due to the piezopotentials. Calculation shows a small piezopotential (several mV) causes a prominent change in T_p. It can be foreseen that this phenomenon will find potential applications in nanoscale strain sensors.

[1] J. P. Gambino, W. D. Kingery, G. E. Pike, H. R. Philipp, and L. M. Levinson, "GRAIN-BOUNDARY ELECTRONIC STATES IN SOME SIMPLE ZNO VARISTORS," Journal of Applied Physics **61**, 2571-2574 (1987).
[2] Y. Qin, X. Wang, and Z. L. Wang, "Microfibre-nanowire hybrid structure for energy scavenging," Nature **451**, 809-813 (2008).
[3] L. Li, "Electromechanically tuned resistive switching device," Applied Physics Letters **103** (2013).
[4] R. Kumar, O. Al-Dossary, G. Kumar, and A. Umar, "Zinc Oxide Nanostructures for NO2 Gas–Sensor Applications: A Review," Nano-Micro Letters **7**, 97-120 (2015).
[5] B. Kumar and S.-W. Kim, "Energy harvesting based on semiconducting piezoelectric ZnO nanostructures," Nano Energy **1**, 342-355 (2012).
[6] W.-J. Ong, S.-Y. Voon, L.-L. Tan, B. T. Goh, S.-T. Yong, and S.-P. Chai, "Enhanced Daylight-Induced Photocatalytic Activity of Solvent Exfoliated Graphene (SEG)/ZnO Hybrid Nanocomposites toward Degradation of Reactive Black 5," Industrial & Engineering Chemistry Research **53**, 17333-17344 (2014).
[7] L. Li, T. Zhai, Y. Bando, and D. Golberg, "Recent progress of one-dimensional ZnO nanostructured solar cells," Nano Energy **1**, 91-106 (2012).
[8] K. Zhang, Y. Zhang, T. Zhang, W. Dong, T. Wei, Y. Sun, X. Chen, G. Shen, and N. Dai, "Vertically coupled ZnO nanorods on MoS2 monolayers with enhanced Raman and photoluminescence emission," Nano Research **8**, 743-750 (2015).
[9] P. Lin, X. Chen, X. Yan, Z. Zhang, H. Yuan, P. Li, Y. Zhao, and Y. Zhang, "Enhanced photoresponse of Cu2O/ZnO heterojunction with piezo-modulated interface engineering," Nano Research **7**, 860-868 (2014).
[10] Z. L. Wang, "Nanopiezotronics," Advanced Materials **19**, 889-892 (2007).
[11] Y. Zhang, Y. Liu, and Z. L. Wang, "Fundamental Theory of Piezotronics," Advanced Materials **23**, 3004-3013 (2011).
[12] Y. Liu, Y. Zhang, Q. Yang, S. Niu, and Z. L. Wang, "Fundamental theories of piezotronics and piezo-phototronics," Nano Energy.
[13] J. Gao, J. M. Luther, O. E. Semonin, R. J. Ellingson, A. J. Nozik, and M. C. Beard, "Quantum Dot Size Dependent J-V Characteristics in Heterojunction ZnO/PbS Quantum Dot Solar Cells," Nano Letters **11**, 1002-1008 (2011).
[14] S. Haffad, G. Cicero, and M. Samah, "Structural and electronic properties of ZnO nanowires: a theoretical study," Energy Procedia **10**, 128-137 (2011).
[15] S. M. Sze and K. K. Ng, *Physics of Semiconductor Devices* (Wiley, 2006).
[16] B. J. Coppa, C. C. Fulton, P. J. Hartlieb, R. F. Davis, B. J. Rodriguez, B. J. Shields, and R. J. Nemanich, "In situ cleaning and characterization of oxygen- and zinc-terminated, n-type, ZnO{0001} surfaces," Journal of Applied Physics **95**, 5856-5864 (2004).
[17] B. J. Coppa, C. C. Fulton, S. M. Kiesel, R. F. Davis, C. Pandarinath, J. E. Burnette, R. J. Nemanich, and D. J. Smith, "Structural, microstructural, and electrical properties of gold films and Schottky contacts on remote plasma-cleaned, n-type ZnO{0001} surfaces," Journal of Applied Physics **97**, 103517 (2005).
[18] C.-Y. Chen, J. R. D. Retamal, I. W. Wu, D.-H. Lien, M.-W. Chen, Y. Ding, Y.-L. Chueh, C.-I. Wu, and J.-H. He, "Probing Surface Band Bending of Surface-Engineered Metal Oxide Nanowires," Acs Nano **6**, 9366-9372 (2012).
[19] Y. Yang, W. Guo, X. Wang, Z. Wang, J. Qi, and Y. Zhang, "Size Dependence of Dielectric Constant in a Single Pencil-Like ZnO Nanowire," Nano Letters **12**, 1919-1922 (2012).
[20] J. Goldberger, D. J. Sirbuly, M. Law, and P. Yang, "ZnO nanowire transistors," Journal of Physical Chemistry B **109**, 9-14 (2005).
[21] L. Li, "Electromechanical resistive switching via back-to-back Schottky junctions," AIP Advances **5**, 097138 (2015).
[22] Y. Ando and T. Itoh, "Calculation of Transmission Tunneling Current across Arbitrary Potential Barriers," Journal of Applied Physics **61**, 1497-1502 (1987).
[23] R. Tsu and L. Esaki, "Tunneling in a finite superlattice," Applied Physics Letters **22**, 562-564 (1973).
[24] Z. L. Wang and J. Song, "Piezoelectric Nanogenerators Based on Zinc Oxide Nanowire Arrays," Science **312**, 242-246 (2006).
[25] Z. Ren and Y. Rusen, "Separation of the piezotronic and piezoresistive effects in a zinc oxide nanowire," Nanotechnology **25**, 345702 (2014).
[26] O. Pinaud, "Transient simulations of a resonant tunneling diode," Journal of Applied Physics **92**, 1987-1994 (2002).